Image processing in the BRITE nano-satellite mission*

Adam Popowicz[a], PHOTT[b], and BEST[c]

[a]Institute of Automatic Control, Silesian University of Technology, Akademicka 16, Gliwice, Poland
[b]BRITE Photometric Team†
[c]BRITE Executive Scientific Team‡

ABSTRACT

The BRITE nano-satellite mission is an international Austrian-Canadian-Polish project of six small space telescopes measuring photometric variability of the brightest stars in the sky. Due to the limited space onboard and the weight constraints, the CCD detectors are poorly shielded and suffer from proton impact. Shortly after the launch, various CCD defects emerged, producing various sources of impulsive noise in the images. In this paper, the methods of BRITE data-processing are described and their efficiency evaluated. The proposed algorithm, developed by the BRITE photometric team, consists of three main parts: (1) image classification, (2) image processing with aperture photometry and (3) tunable optimization of parameters. The presented pipeline allows one to achieve milli-magnitude precision in photometry. Some first scientific results of the mission have just been published.

Keywords: nano-satellites, photometry, image processing, proton radiation

1. INTRODUCTION

The BRITE Constellation consists of six nano-satellites, built by a consortium from three countries: Poland, Canada and Austria. Each country funded two satellites. Their mission is aimed at observations of the brightest stars in the sky from Low Earth Orbit (600-800 km). The main goal is high-precision, long-term photometry, which is difficult to obtain from ground-based observatories, mainly because there are too few appropriate reference stars for differential photometry. The long time-baseline lightcurves with milli-magnitude precision provided by the BRITE satellites have already allowed study of the oscillation and other properties of observed stars.[1–3] The satellites include either a blue or a red filter, thus providing two-color photometry. The details of the BRITE Constellation satellites are given in Tab. 1.

All the BRITEs share the same basic design presented in detail by Weiss et al.[4] The satellites are equipped with the following instruments: CCD scientific camera, APS (active pixel sensor) star tracker, reaction wheels, Sun sensors, UHF and S-band antennas, solar cells, magnetorquers and on-board computers. The main camera houses a Kodak interline CCD detector KAI 11002M (CCD size: 4072(H)×2720(V) pixels, sensor dimensions: 37.25mm×25.7mm, pixel dimensions: 9μm×9μm, pixel saturation charge: 60 000e$^-$). For more details on the construction of the BRITEs, the reader is referred to the work of Weiss et al.[4] and of Pablo et al. (in prep., 2016).

The field of view of the BRITE CCD camera is 24^o × 19^o. The lens system includes 5 or 4 elements, which produces intentionally defocussed point spread functions (PSF[§]), so that they cover several tens of pixels and

* Based on data collected by the BRITE Constellation satellite mission, designed, built, launched, operated and supported by the Austrian Research Promotion Agency (FFG), the University of Vienna, the Technical University of Graz, the Canadian Space Agency (CSA), the University of Toronto Institute for Aerospace Studies (UTIAS), the Foundation for Polish Science & Technology (FNiTP MNiSW), and National Science Centre (NCN).
† Members of PHOTT: B. Pablo, R. Kuschnig, A. Popowicz, T. Ramiaramanantsoa, G. Whittaker & E. Zoclonska
‡ Members of BEST: G. Handler, O. Koudelka, R. Kuschnig, J. Matthews, A. Moffat, P. Orleanski, A. Pigulski, S. Rucinski, R. Smolec, G. Wade, W. W. Weiss, K. Zwintz, D. Baade, C. Neiner, A. Pamyatnykh, A. Popowicz, J. Rowe & A. Schwarzenberg Czerny
E-mail: apopowicz@polsl.pl
§Point spread function - the response of an optical system to a point-like object.

Table 1: BRITE Constellation overview.

Name	Abbreviation	Filter	Launch date	Country
BRITE Austria	BAb	blue	Feb. 25, 2013	Austria
Uni BRITE	UBr	red	Feb. 25, 2013	Austria
BRITE Toronto	BTr	red	June 19, 2014	Canada
BRITE Montreal	BMb	blue	June 19, 2014	Canada
BRITE Lem	BLb	blue	Nov. 21, 2013	Poland
BRITE Heweliusz	BHr	red	Aug. 19, 2014	Poland

depend on the position in the detector's plane (see examples in Fig. 1). The exposures taken by the scientific CCD camera are usually 1 second long, which allow for adequate photometry of stars down to roughly visual magnitude 5. Due to the limited download rate and the high cadence required, only small parts of the images, called rasters (approx. 30×30 pixels, depending on the size of the stellar profile) containing selected stellar objects, are extracted and transmitted to the ground radio stations.

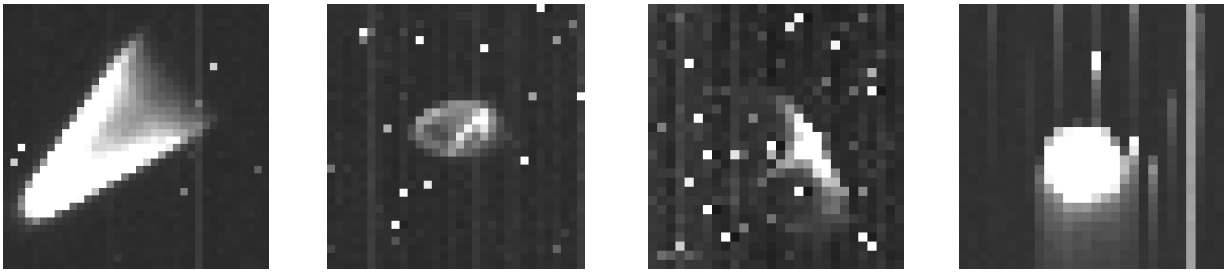

Figure 1: Examples of CCD rasters from BRITE satellites. From the left: BHr, BAb, UBr and BTr (various targets, temperatures and PSF positions within CCD plane). Note impulsive noise in the form of column intensity offsets and plenty of hot pixels. The raster on the right is affected by charge transfer inefficiency.

A drawback of the BRITE nano-satellites is the lack of heavy shielding around the most sensitive part of the imaging system - the CCD sensor. Shortly after the launch of the first BRITE satellites (UniBRITE and BRITE-Austria), so-called hot pixels (HPs) and column defects started to appear. Their presence threatened the mission objective to obtain high-precision photometry. Moreover, the number of HPs is continuously growing as the CCDs are impacted by energetic protons coming mainly from the Sun. Minor modifications were thus introduced compared to the original satellite design in the first BRITEs. As an example, the second Polish satellite (BHr, Heweliusz), was equipped with additional borotron shielding, which allowed for stronger protection from proton impact in orbit. The decision for incorporating this improvement was based on the experience gained from the first year of Austrian satellites in space.

However, the most serious disturbance of images obtained by the BRITEs was charge-transfer inefficiency (CTI[5]). The problem appeared due to shallow defects located just below the pixel electrodes. Large vertical regions of the CCDs were affected, blurring significantly each hot pixel and stellar profile as depicted in the right-most raster of Fig. 1. Fortunately this phenomenon was successfully removed by reducing the frequency of the vertical clock in the CCDs, so that the electrons have more time to be transferred between pixels. Such a slowing of vertical transfer of charge did not changed any of CCD parameters (gain, dark current, or readout noise). The readout time also remained nearly the same, since it depends mainly on the clocking of horizontal register.

2. ALGORITHM

The proposed algorithm for reduction of BRITE data can be divided into three main parts: image classification (A), image processing with aperture photometry and intrapixel-sensitivity compensation (B), and optimization

of parameters (C). The first part includes the routines developed for finding and rejecting images disturbed by imperfect tracking of a satellite. In this part the dark frames are also retrieved. They are actually pseudo-dark frames obtained by intentional satellite movements by shifting the stars from their initial positions to reveal the locations of HPs. The following steps are included in part A:

A1. **correction of column intensity offsets** - subtracting the column median intensities (this was the only way to remove the bias, since there are no pre- or overscan pixels available),
A2. **simple denoising** - applying 3×3 median filtering, (each image pixel is replaced by the median of 9 pixels in the local sliding window),
A3. **specifying the star region (star mask, SM)** - thresholding the filtered image at 100 ADU[¶] (this value was chosen arbitrarily after inspection of all stars in the test data sets; it is close to the background bias level),
A4. **stellar profile masking** - steps A1-A3 are repeated using the image with the SM region masked to avoid including PSF pixels in the estimation of column intensity offset . The process is iterated as long as the number of detected PSF pixels increases.
A5. **specifying the stellar area (S_a)** - counting all the pixels within the SM,
A6. **defining the range of proper S_a values** - manually inserting lower and upper thresholds (T_{high}, T_{low}) based on the visual assessment of the time dependence of S_a,
A7. **classifying images** - dividing the set of images into proper ($T_{high} > S_a > T_{low}$), dark ($S_a = 0$), and rejected ($T_{high} < S_a$ or $T_{low} > S_a > 0$) frames.

The next part (B) of the algorithm contains a set of procedures aimed at determining the total flux for an observed star. Only the images classified previously as proper are considered. The dark frames are median-averaged to create the master dark frame, in which the pixels are classified as HPs if their intensity is above a specified threshold T_{bad} (this parameter is optimized in part C). This gives the mask of bad pixels utilized in the interpolation phase. The following steps are included in part B of the pipeline:

B1. **defining the star regions** - steps A1-A4 are repeated to obtain the star mask (SM),
B2. **estimating the star centroid position** - the centroid (center of gravity) of the PSF is calculated using partially processed image, i.e. that with compensated column intensity offsets, masked by the SM, and with only detected HPs replaced by the median of their neighbors,
B3. **replacement of hot pixels** - as the centroids are initially estimated, the HPs are interpolated by a complex routine which utilizes the information of pixel intensities in previous and following images obtained during the orbit, (100 minutes, 40-60 measurements per orbit). Note that even sophisticated interpolation methods, like those presented by Popowicz et al.[6], were unable to estimate precisely the intensity of HPs due to the strong undersampling and complexity of PSF profiles. Therefore, a novel approach was proposed: First, (1) the centroid of currently filtered image is estimated and then (2) the shift S_{HP} of a given hot pixel is obtained relatively to the centroid. Next, (3) the centroids are estimated in all other images in an orbit. Finally, (4) the algorithm averages the intensities of pixels located with the same shift S_{HP} relatively to the PSF centroids. In such an averaging, obviously, only the pixels not included in the HP mask are considered.
B4. **circular aperture photometry** - in the final filtered image the charge is counted within the circular aperture determined around the star centroid (the aperture includes pixels having distances between their centers and the centroid smaller than the specified radius R, optimized in part C). Since stellar profiles show various shapes, frequently changing with temperature, a simple circular aperture was chosen as a trade-off.
B5. **compensation of intrapixel sensitivity variations** - due to the nonuniform sensitivity of pixels across their surface and because of the high intensity gradients in PSFs, the impact of intrapixel sensitivity variations needs to be compensated. It is preformed by decorrelation of the magnitude error (computed as a deviation from the median magnitude in orbit) plotted as a function of centroid position modulo one.

The last part (C) of the algorithm is actually the loop which involves part B run with different hot pixel thresholds T_{bad} and employing various aperture radii R. To assess the lightcurve quality, the median absolute

[¶]ADU stands for Analog-to-Digital Units (1 ADU is approximately 3.4 electrons in BRITE CCDs).

deviation of results is obtained in each satellite orbit (MAD_i). The robust, final quality measure (Q_m), is the median of normalized MADs, defined as follows:

$$Q_m = \mathrm{median}\left\{\frac{\mathrm{MAD}_i}{\sqrt{N_i}}\right\}, \tag{1}$$

where MAD_i and N_i denote the median absolute deviation from median magnitude in orbit and the number of measurements in the i-th orbit, respectively. The median-based statistics were employed due to the presence of outliers and orbits corrupted by stray light and by star-tracker instabilities. The normalization by a factor of $\sqrt{N_i}$ reflects the noise reduction provided by the averaging. An example of a final optimization curve for a sample star (HD 36861) is presented in Fig. 2. For this particular target, which does not show any intrinsic variations within the time scale of a single orbit, the best photometric precision was achieved for $T_{bad} = 150$ ADU and $R = 7$. For $R > 7$ the pixels not belonging to the star profile were included in the aperture, enlarging the impact of readout noise. It should be also noted that increasing T_{bad} to 200 ADU or reducing it to 100 ADU resulted in decrease of the quality of the final photometry. The optimal value of $T_{bad} = 150$ ADU should therefore be understood as a trade-off between too many HPs (low performance of interpolation) or too few of them detected (photometric drifts due to the dark current) included in the mask of bad pixels.

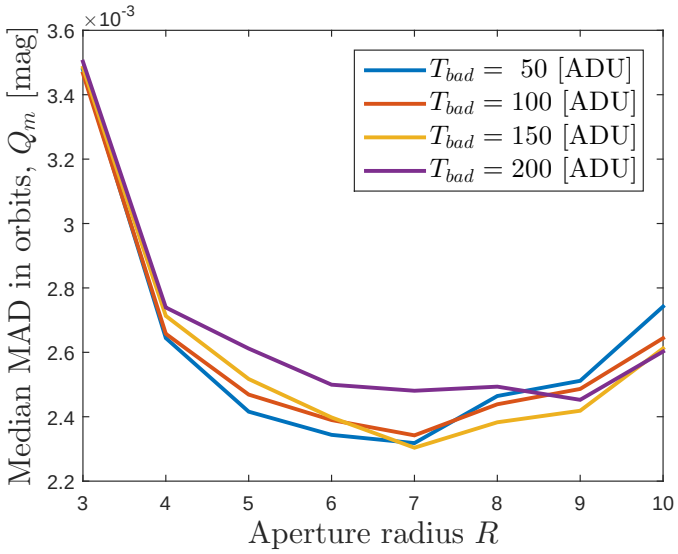

Figure 2: The optimization curves for HD 36861, UBr satellite.

3. PHOTOMETRIC QUALITY

The quality of the photometry was compared with the theoretical limits dictated by a combination of the Poisson distribution of counts, dark current and the readout noise. The required CCD calibration was performed during the pre-launch ground-based laboratory tests. The resulting values of gain, dark current generation rate and readout noise for discrete temperature values, are provided in Tab. 2. For a required temperature, the parameters were obtained by linear interpolation.

Table 2: BRITE CCD characteristics measured on the ground.

Temperature (^{o}C)	-20	0	10	20	30	60
Gain (e^- ADU^{-1})	3.43	3.42	3.49	3.44	3.40	3.60
Dark current generation rate (e^- s^{-1} pixel^{-1})	0	2	8	21	49	534
Readout noise (e^- pixel^{-1})	13	13	14	16	19	63

Knowing the aperture radius (R), registered number of photons (I_f), dark current rate (I_d) and readout noise (σ_r), one can define the limiting standard deviation of the resulting photometry (i.e. the product of averaging of N measurements in each orbit):

$$\sigma_{limit} = -2.5\log_{10}\left(\frac{\sqrt{I_f + \pi R^2 I_d + \pi R^2 \sigma_r^2}}{I_f}\right) \cdot \frac{1}{\sqrt{N}} \quad [\text{mag}]. \tag{2}$$

On the other hand, to estimate the actual standard deviation of real data, the previously introduced quality measure Q_m can be employed:

$$\sigma_{real} = 1.4826 \cdot Q_m \tag{3}$$

The usage of such median-based quality assessment was necessary to reduce the impact of orbits corrupted by star-tracker instabilities, and to suppress the influence of outliers on σ. The known relation between the standard deviation and MAD ($\sigma = 1.4826 \cdot \text{MAD}$[7]) was justified since the photometric points within orbits follow a normal distribution.

The comparison of actual and estimated limiting photometric accuracy for the first field (Orion, 2013) observed by the first two launched satellites (BAb and UBr), is depicted in Fig. 3. This particular field was investigated starting from Oct 1, 2013 through about 5 months. Note that UBr and BAb spent over 7 months in orbit before the start of observations of the Orion field, so that the scientific CCDs were already significantly damaged by protons. Moreover, the sensor temperatures ranged from 5°C to nearly 40°C during this observation run. Therefore, the retrieved images can be considered as a representative, if not extreme, data set produced by the BRITE Constellation.

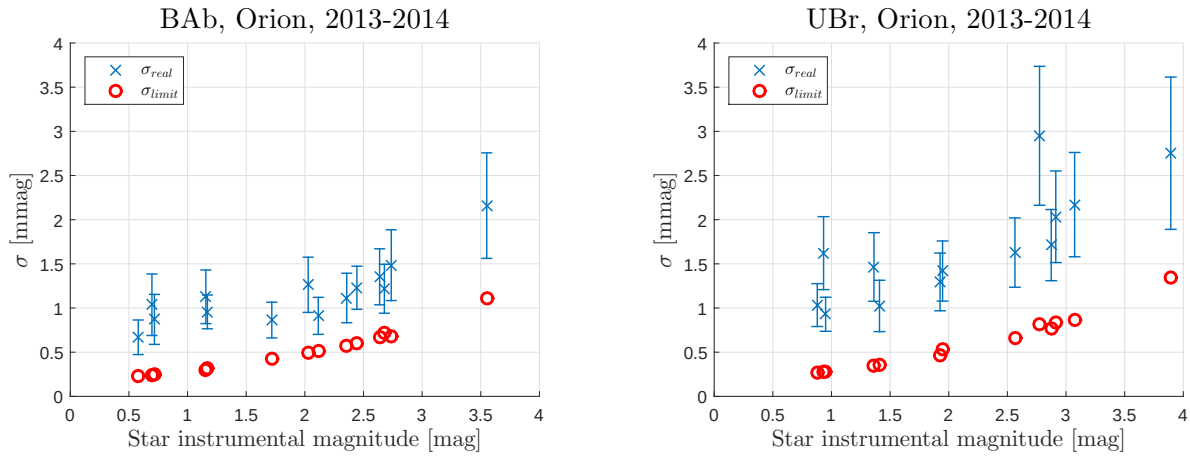

Figure 3: Comparison of limiting (σ_{limit}) and actual (σ_{real}) photometric accuracy for stars in the first field, Orion, observed by the first two launched satellites: BAb (left) and UBr (right). The blue error bars depict the spread of σ_{real} results among the orbits as calculated using robust estimator of standard deviation: $1.4826 \cdot \text{MAD}$. Small levels of intrinsic stellar variability over 20 minutes could slightly raise the observed scatter in some cases.

The limiting accuracy is noticeably better than the measured performance. On average, the spread of points was twice that estimated by theoretical calculations. The origin of this situation is likely related mainly to the proton-induced defects in the CCDs. The residual noise, even after strong suppression by the procedures incorporated in the processing pipeline, leaves significant potential correlations of photometric outcomes with the following instrumental parameters: temperature, stellar profile centroid and orbital phase. This biasing has to be compensated by proper decorrelation techniques, which are not included in the standard pipeline. However, a possible approach to the decorrelation of BRITE data has already been presented by Pigulski et al.[2] A more detailed insight into the reasons for residual errors is listed below.

1. The interpolation of HP intensity is always burdened with some degree of uncertainty.

2. Despite the use of an image classification algorithm, some frames are still degraded by minor star-tracker instabilities. Such blurred images reduce the interpolation efficiency and introduce flux underestimation in constant, circular apertures.
3. The employed procedure of hot pixel detection is based on dark charge-thresholding. Unfortunately, the dark-current distribution covers both low and high intensities (an exponential dependency of dark charge can be observed). Therefore, there will be a fraction of faulty pixels which will not be included in the hot pixel mask but will affect the measurements. Unfortunately, the selection of HPs is always a trade-off: too many detected HPs will reduce the interpolation quality, while too few of them will introduce RTS noise and temperature related drifts into the final lightcurves.
4. A circular aperture does not always fit well the PSF shape, which sometimes results in including pixels without any light detected or excluding some which are within the PSF region.
5. The dark current, estimated during the laboratory tests, has increased significantly in orbit. Thus, the limitations of photometric precision (σ_{limit}) should be understood rather as the noise floor of the BRITE photometric system perfectly protected from proton impact.
6. Despite the fact that the stellar profiles cover tens of pixels, the total noise may be slightly elevated by sensitivity differences between the pixels. However it strongly depends on the intensity distribution within PSF and therefore it was not included in the noise budget presented in this paper.

4. SUMMARY

Precision photometry of stellar objects is the main goal of the BRITE nano-satellites. Unfortunately, soon after the launch of the first two satellites, proton-induced defects appeared on the CCDs, complicating the mission and making the image processing a challenging task. The defects appeared in the form of hot pixels and biasing of CCD columns due to the extensive generation of dark current. Also, the charge transfer inefficiency affected large regions of the CCDs. Fortunately, this problem was solved by reduction of the frequency of the readout clock.

In this paper a method for the reduction of BRITE data is presented. The algorithm consists of three main parts: image classification, image processing and optimization of parameters. While the first stage allows for rejecting frames degraded by star-tracker instabilities, the remaining stages aim at precise aperture photometry of observed objects. Thanks to various pipeline steps, like the iterative compensation of column intensity offsets, a dedicated technique of hot-pixel interpolation and compensation of intrapixel sensitivity variations, the intensity dispersion of photometric points is not far from the required milli-magnitude regime. Importantly, the achieved accuracy after decorrelations has facilitated the presentation of the first viable scientific outcomes of the mission.[1–3] A more detailed and complete version of this paper is in preparation and will be published soon.

A new mode of observation, called chopping, is currently implemented in the BRITE satellites. In this mode, consecutive images are recorded with shifts of the order of a couple of PSF widths in one direction (back and forth, between exposures). This allows one to identify the position of hot pixels and better characterize and mitigate their thermal activity. A dedicated pipeline is being developed for this observation mode. Such an upgrade leads to better photometry of faint objects even with strongly degraded detectors (i.e., after several years of work in space).

ACKNOWLEDGMENTS

Adam Popowicz was supported by the Polish National Science Center, grant no. 2013/11/N/ST6/03051: Novel Methods of Impulsive Noise Reduction in Astronomical Images. The computations were performed using the infrastructure supported by POIG.02.03.01-24-099/13 grant: GeCONiI - Upper Silesian Center for Computational Science and Engineering. The Polish BRITE team acknowledges PMN grant 2011/01/M/ST9/05914.

The first author would like to express particular thanks for the opportunity of giving this review and for numerous comments provided by Andrzej Pigulski, Gregg Wade, Tony Moffat and Werner W. Weiss.

REFERENCES

[1] Weiss, W. W., Frhlich, H.-E., Pigulski, A., Popowicz, A., Huber, D., Kuschnig, R., Moffat, A. F. J., Matthews, J. M., Saio, H., Schwarzenberg-Czerny, A., Grant, C. C., Koudelka, O., Lftinger, T., Rucinski, S. M., Wade, G. A., Alves, J., , et al., Guedel, M., Handler, G., Mochnacki, St., Orleanski, P., Pablo, B., Pamyatnykh, A., Ramiaramanantsoa, T., Rowe, J., Whittaker, G., Zawistowski, T., Zocoska, E., and Zwintz, K., "The roAp star circinus as seen by BRITE-Constellation," *Astronomy & Astrophysics* **588**, A54 (2016).

[2] Pigulski, A., Cugier, H., Popowicz, A., Kuschnig, R., Moffat, A. F. J., Rucinski, S. M., Schwarzenberg-Czerny, A., Weiss, W. W., Handler, G., Wade, G. A., Koudelka, O., Matthews, J. M., Mochnacki, St., Orleaski, P., Pablo, H., Ramiaramanantsoa, T., Whittaker, G., Zocoska, E., and Zwintz, K., "Massive pulsating stars observed by BRITE-Constellation," *Astronomy & Astrophysics* **588**, A55 (2016).

[3] Baade, D., Rivinius, Th., Pigulski, A., Carciofi, A. C., Martayan, Ch., Moffat, A. F. J., Wade, G. A., Weiss, W. W., Grunhut, J., Handler, G., Kuschnig, R., Mehner, A., Pablo, H., Popowicz, A., Rucinski, S., and Whittaker, G., "Short-term variability and mass loss in Be stars," *Astronomy & Astrophysics* **588**, A56 (2016).

[4] Weiss, W. W., Rucinski, S. M., Moffat, A. F. J., Schwarzenberg-Czerny, A., Koudelka, O. F., Grant, C. C., Zee, R. E., Kuschnig, R., Mochnacki, S., Matthews, J. M., Orleanski, P., Pamyatnykh, A., Pigulski, A., Alves, J., Guedel, M., Handler, G., Wade, G. A., and Zwintz, K., "BRITE-Constellation: Nanosatellites for Precision Photometry of Bright Stars," *PASP* **126**, 573–585 (June 2014).

[5] Janesick, J. R., [*Scientific charge-coupled devices*] (2001).

[6] Popowicz, A., Kurek, A. R., and Filus, Z., "Bad Pixel Modified Interpolation for Astronomical Images," *PASP* **125**, 1119–1125 (Sept. 2013).

[7] Rousseeuw, P. J. and Croux, C., "Alternatives to the median absolute deviation," *Journal of the American Statistical Association* **88**(424), 1273–1283 (1993).